

Structural and thermal properties of boron nitride nanoparticles

V. Salles^a, S. Bernard^{b,*}, R. Chiriac^a, P. Miele^b

^a Laboratoire des Multimatériaux et Interfaces (UMR CNRS 5615), Université de Lyon, Université Lyon1, 43 bd du 11 Novembre 1918, 69622 Villeurbanne Cedex, France

^b Institut Européen des Membranes (UMR CNRS 5635) IEM/Université Montpellier 2 - CC047 - Place E. Bataillon, 34095 Montpellier Cedex 5, France

Available online 25 September 2011

Abstract

In the present study, our main motivation was to investigate the structural and thermal stability of BN nanoparticles ($B_{1.0}N_{0.9}$ -NPs) produced by spray-pyrolysis (SP) of borazine at 1400 °C by thermogravimetric experiments and X-ray diffraction. We observed that $B_{1.0}N_{0.9}$ -NPs are relatively stable in air below 850 °C in which only oxidation of the NP surface proceeded. Above 850 °C, the powders started to strongly react with air due to bulk oxidation. Under nitrogen, they appeared to be less stable than plate-like BN synthesized from borazine at 1400 °C through conventional pyrolysis. This is related to the low degree of crystallization of $B_{1.0}N_{0.9}$ -NPs that clearly affects their stability. Using a post-pyrolysis treatment at 1400 °C, $B_{1.0}N_{0.9}$ -NPs remained stable up to 1600 °C similarly to plate-like BN. However, above 1600 °C, a relatively fast weight loss occurred for $B_{1.0}N_{0.9}$ -NPs, whereas plate-like BN remained stable up to 1800 °C. This indicated that their lower size also affects their high temperature thermal behavior.

© 2011 Elsevier Ltd. All rights reserved.

Keywords: Boron nitride; Nanoparticles; Borazine; Spray-pyrolysis; Thermal stability

1. Introduction

Hexagonal boron nitride (BN) has received considerable attention according to its unique physical and chemical properties.^{1,2} The layered lattice structure of BN provides good lubricating properties; it is not wetted by most molten metals, glasses and salts and hence it has a high resistance to chemical attack; it displays high dielectric breakdown strength, high volume resistivity and good resistance to oxidation. Based on such properties, it displays extensive applications in fields ranging from optical storage to medical treatment, photocatalysis, optoelectronic devices, and electrical insulation. BN also has a high thermal conductivity and excellent high temperature resistance which combined to a low density render it an appropriate candidate for the most recent electronic devices, communication equipment and lighting apparatuses. However, BN particles produced at industrial scales still have a plate-like shape. Considering the low filling density and poor processability of plate-like BN, it is desirable to synthesize BN nanoparticles with small and uniform particle size. This could permit a much higher

loading density in plastics or resins used in electronic devices to optimize the dissipation of heat while keeping processability of the nanocomposites. The preparation of BN nanoparticles has already been reported in the literature.^{3–11} In particular, we have proposed a simple and cost-effective one-step access to BN nanoparticles ($B_{1.0}N_{0.9}$ -NPs) via the SP of borazine under nitrogen at 1400 °C.¹¹ Here, the aim of the present study is to focus on the thermal stability of $B_{1.0}N_{0.9}$ -NPs by high-temperature TG experiments under air and nitrogen and to determine the effect of the final temperature on their structure by XRD. The literature contains numerous studies of BN oxidation^{12–25} but the thermal stability of BN nanoparticles has never been studied up to now.

2. Experimental procedure

2.1. Post-pyrolysis treatments of $B_{1.0}N_{0.9}$ -NPs

The process describing the preparation of $B_{1.0}N_{0.9}$ -NPs is thoroughly discussed in our previous paper.¹¹ To study the evolution of their crystallization degree, $B_{1.0}N_{0.9}$ -NPs were annealed in a graphitic furnace (Gero Model HTK 8) under nitrogen at 10 °C/min up to the desired temperature (in the range 1400–1800 °C) with a holding time of 1 h, before cooling down to RT at 10 °C/min.

* Corresponding author.

E-mail address: Samuel.Bernard@iemm.univ-montp2.fr (S. Bernard).

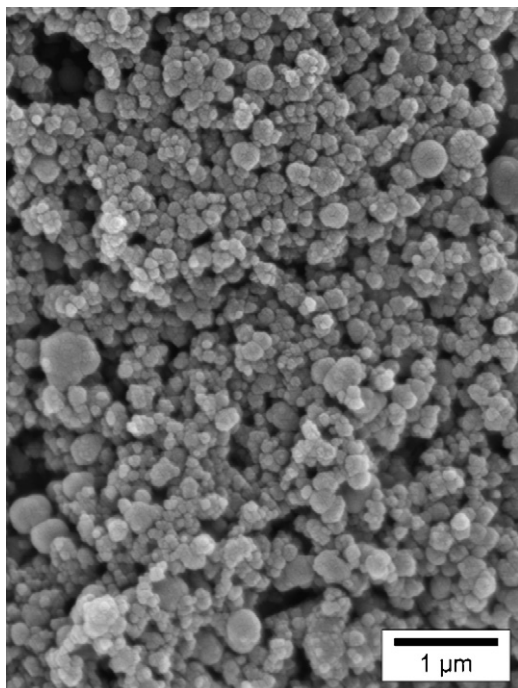


Fig. 1. SEM picture of B_{1.0}N_{0.9}-NPs.

2.2. Characterization

B_{1.0}N_{0.9}-NPs have been firstly studied by thermogravimetric analyses in dry air (HT-TGA, Mettler Toledo TGA/SDTA 851 equipment; Impurity in H₂O: 2000 ppm) in the dynamic mode from RT to 1000 °C using platinum crucibles and horizontal alumina sample holder. Samples were heat-treated with a heating rate of 5 °C/min to 1000 °C and kept at this temperature for 10 min, then cooling down to RT at 20 °C/min. The same experiments were made in isothermal modes at different temperatures starting from 300 to 1000 °C. Samples were heated at a heating rate of 5 °C/min to the desired temperature and kept at this temperature for 5 h, then cooling down at 20 °C/min. Then, B_{1.0}N_{0.9}-NPs were studied by high-temperature thermogravimetric analysis (HT-TGA, Setaram Setsys evolution TGA equipment) (800–1800 °C; heating rates: 10 °C/min) using tungsten crucibles in a nitrogen atmosphere. In parallel, the characterization of the nanoparticles annealed in the temperature range 1400–1800 °C was carried out by powder X-ray diffraction (XRD, with Cu K α radiation PANalytical PW 3040/60 X'Pert PRO X-ray diffraction system).

3. Results and discussion

Recently, we successfully demonstrated that B_{1.0}N_{0.9}-NPs with a relatively low crystallization degree could be obtained by the SP of borazine at 1400 °C in a nitrogen atmosphere (Fig. 1).¹¹

We speculated that the poor crystallinity of the BN phase and/or the small size of powders may affect the thermal stability of these nanomaterials, and therefore their application. In order to provide information on their thermal stability, we investigated the thermal behavior of B_{1.0}N_{0.9}-NPs in air up to 1000 °C (in

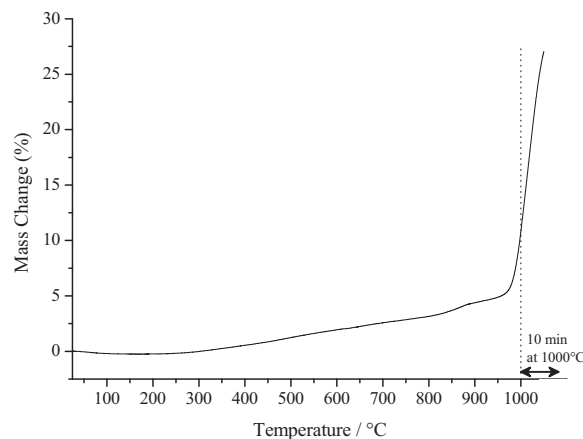


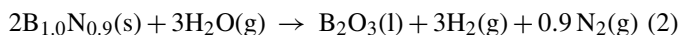
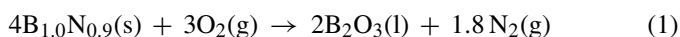
Fig. 2. HT-TGA of B_{1.0}N_{0.9}-NPs (RT–1000 °C, dry air, $P = 1$ atm).

dynamic and isothermal modes), then in a nitrogen atmosphere up to 1800 °C.

3.1. HT-TGA of B_{1.0}N_{0.9}-NPs

3.1.1. Thermal behavior under air

It is known that BN is oxidized into boric oxide when exposed to oxygen and moisture at intermediate temperatures (800–900 °C).^{12–26} In the case of B_{1.0}N_{0.9}-NPs, it would result in the formation of boric oxide according to Eqs. (1) and (2).



It should be mentioned that NO₂ (g) may form as a by-product as well.¹⁶

In order to elucidate the thermal behavior of B_{1.0}N_{0.9}-NPs at high temperatures, thermogravimetric analyses were first conducted under dry air ($P = 1$ atm) in a dynamic mode from RT to 1000 °C (Fig. 2).

In the absence of moisture, boron nitride is known to be stable up to 800 °C.^{23,24} Here, we observed that B_{1.0}N_{0.9}-NPs remained stable up to 250 °C, temperature from which the weight continuously increased up to 850 °C (3.7 wt%). A second weight gain occurred from 850 to 960 °C (1.5 wt%) and a third step corresponded to a fast weight loss at 960 °C to reach a total weight gain of 27 wt% at 1000 °C. We can identify two regimes of oxidation: a first from 250 to 850 °C concerning the reaction of oxygen with the NP surface probably forming a passivating boron oxide layers which acts as a protective coating (because it is solid with a density of 1.85 g/cm³ up to 410 °C, then becoming liquid with a density of 2.46 g/cm³)²⁵ and a second regime in the temperature range 850–1000 °C where either oxidation of the bulk particles proceeded by diffusion of oxygen through liquid boron oxide^{23,24} or interface reaction²³ occurred between the boron oxide layer and the particle. Under isothermal mode (dwelling time of 5 h, Fig. 3), it is clear that oxidation process remained slow below 800 °C (low weight gain), whereas a larger two-step weight gain occurred above and especially at 900 °C. Isothermal TGA curves allowed

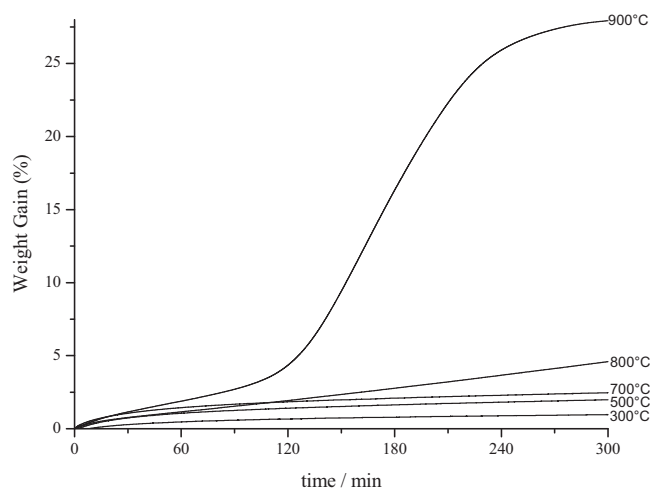


Fig. 3. Isothermal HT-TGA of $B_{1.0}N_{0.9}$ -NPs (dry air, $P = 1$ atm).

distinguishing the two oxidation regimes: a first domain with a poor weight gain most probably resulting from an induction time due to oxidation of the NPs surface, followed by a second domain with a faster weight gain due to bulk oxidation. It is interesting to observe that the weight gain (32.5 wt%) of $B_{1.0}N_{0.9}$ -NPs ($d_{002} = 3.68$ Å) recorded at 900 °C is considerably higher than those found for BN specimens with different interplanar distance from 3.33 Å (+5 wt%) to 3.67 Å (+22 wt%) after exposure to dry air at 950 °C for 3 h.¹⁹ In the latter case, oxidation reaction reach a plateau after 3 h of exposure to dry air.

3.1.2. Thermal behavior under nitrogen

The high-temperature behavior of as-prepared $B_{1.0}N_{0.9}$ -NPs was then investigated by HT-TGA under nitrogen in the 450–1800 °C temperature range (Fig. 4) to assess the thermal stability and the overall weight changes which occur.

Data were compared with those corresponding to home-made plate-like BN particles prepared via a multi-step process from borazine and derived polyborazylene at 1400 °C under nitrogen

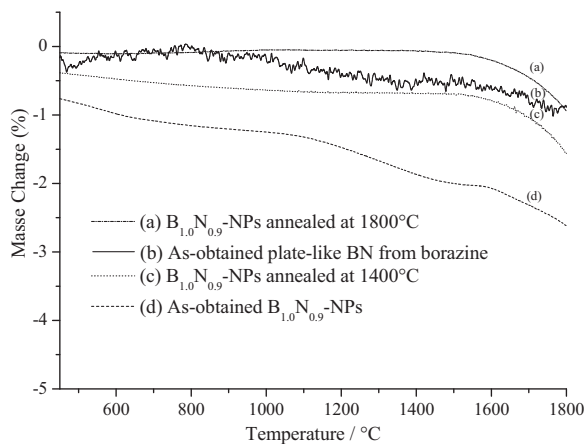


Fig. 4. HT-TGA of $B_{1.0}N_{0.9}$ -NPs (450–1800 °C, N_2 atmosphere), post-treated at 1400 °C and 1800 °C and compared with plate-like BN produced from borazine at 1400 °C.

similar to the process described in Ref.²⁷ It was shown that $B_{1.0}N_{0.9}$ -NPs exhibited a quasi-continuous weight loss up to 1100 °C (1.3 wt%). A heat treatment at temperatures higher than 1600 °C resulted in a two-step decomposition associated with a final weight loss measured at 1800 °C of 2.7 wt%. In comparison, plate-like BN particles obtained from the same molecular precursor at the same final temperature demonstrated stability over the considered temperature range. As a consequence, we suggested that the weight loss between 200 and 1100 °C could be assigned in a major part to the evolution of H_2 due to a remaining part of hydrogen in $B_{1.0}N_{0.9}$ -NPs explained by uncompleted borazine decomposition during SP. It is in good agreement with the chemical analysis experiment performed on $B_{1.0}N_{0.9}$ -NPs in a previous study giving hydrogen content lower than 1 wt%.¹¹ This hypothesis was confirmed by the TGA performed on the same NPs after annealing at 1400 °C for 2 h (Fig. 4), simulating the heat-treatment to prepare plate-like BN. In these conditions, the behavior of these “post-treated” $B_{1.0}N_{0.9}$ -NPs is very close to that of the plate-like BN up to 1600 °C but remained similar to that of the starting NPs for higher temperatures. This is also the case of $B_{1.0}N_{0.9}$ -NPs post-treated at 1800 °C: they systematically showed decomposition above 1600 °C.

The thermally induced degradation of the material at elevated temperatures is usually a function of chemical composition, crystallization state and surrounding atmosphere. In the present article, a first important issue of the lack of stability of $B_{1.0}N_{0.9}$ -NPs lies in their crystalline perfection. Studies of BN have demonstrated that the crystalline perfection of the BN phase is mainly controlled by the final temperature of the process and that temperatures above 1400 °C need to be applied to crystallize the BN phase.^{27–31} The extremely fast heating rate involved by SP ($\sim 10^2$ °C/s), and the short residence time at 1400 °C (3 s) justifies the low crystallization degree of $B_{1.0}N_{0.9}$ -NPs. This clearly explains the relatively fast and strong weight change above 850 °C during TG experiments. A second important issue of the lack of stability of $B_{1.0}N_{0.9}$ -NPs probably comes from their small size. Indeed, recent publications showed that the decrease of the size of micropowders strongly reduced the thermal stability of bulk materials in a nitrogen environment.³² Decreasing the particle size from values >315 μm to values <32 μm involved a shift in the temperature of thermal decomposition in a nitrogen environment from 1900 °C to 1680 °C for SiBCN phases. This is confirmed in our study by comparing the thermal stability under nitrogen of $B_{1.0}N_{0.9}$ -NPs and plate-like BN particles and also by comparing the oxidation behavior under isothermal conditions of $B_{1.0}N_{0.9}$ -NPs and that of BN specimens¹⁹ for a similar interplanar distance. According to the work of Economy et al.,¹⁹ the weight gain of $B_{1.0}N_{0.9}$ -NPs should be less than 22 wt% ($d_{002} = 3.67$ Å). With a weight gain of 32.5 wt% ($d_{002} = 3.68$ Å) after exposure at 900 °C for 5 h in our case, it is clear that the small size increases the thermal and chemical reactivity of $B_{1.0}N_{0.9}$ -NPs. A third important issue of the lack of stability of $B_{1.0}N_{0.9}$ -NPs concerns the specific surface area which should be as low as possible. The BET specific surface area (SSA) of $B_{1.0}N_{0.9}$ -NPs was measured to be 34.6 ± 0.7 m²/g.¹¹

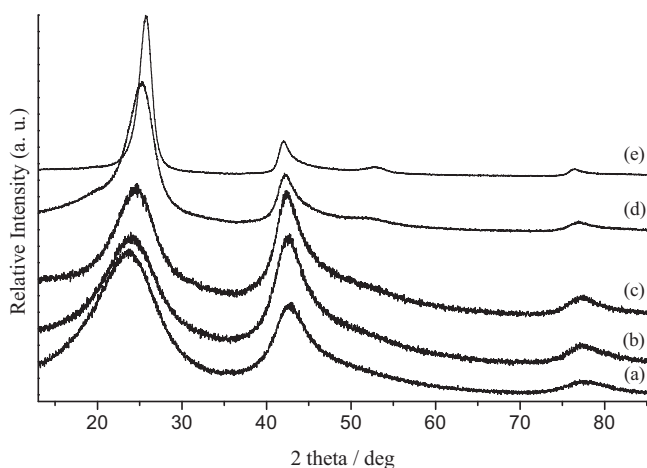


Fig. 5. X-ray diffractograms of as-prepared $B_{1.0}N_{0.9}$ -NPs (a), samples heat treated at 1400 °C (b), 1600 °C (c), 1700 °C (d), and 1800 °C (e).

3.2. Structural changes of $B_{1.0}N_{0.9}$ -NPs during heat-treatment under nitrogen

Structural changes have been monitored by X-ray diffraction (XRD; Fig. 5). Fig. 5 shows the 13–85° X-ray diffractograms recorded at RT for the 1400, 1600, 1700, and 1800 °C heat-treated samples

The XRD patterns of 1400 °C (Fig. 5b) and 1600 °C (Fig. 5c) heat-treated samples do not exhibit any fundamental changes in term of resolution compared to that of as-prepared $B_{1.0}N_{0.9}$ -NPs (Fig. 5a). The corresponding XRD patterns show very broad peaks at the h -BN (002), (100)/(101)/(004) and (110) positions corresponding to nanosized BN. In particular, the (002) peak slightly shifts to lower angles in such samples and the (100), (101) and (004) peaks merge into a single broad peak (Fig. 5a) pointing to the fact that the BN phase remained poorly crystallized and exhibited a turbostratic organization. For the 1700 °C heat-treated sample (Fig. 5d), the (002) peak at 25.30° sharpened indicating that the crystallite size became larger in the c -axis direction, although the shoulder-shaped broad feature remained on the low-angle side of the peak. This was also shown on the sharper (100)/(101)/(004) peak for which it is interesting to observe the gradual separation of the (004) peak from the (100)/(101) peaks. The increase of the heat-treatment temperature to 1800 °C resulted in an increased resolution of the X-ray diffractogram (Fig. 5e). We can clearly distinguish the symmetric (002), (100)/(101), (004) and (110) peak positions. According to the sharpening of the (002) and (100)/(101) peaks, we suggested that the crystallite size continuously increased in the c - and a -axes directions from 1400 to 1800 °C. However, no clear peaks corresponding to (102) and (112) planes were observed. These findings tended to demonstrate that $B_{1.0}N_{0.9}$ -NPs annealed at 1800 °C still have a turbostratic structure. However, it should be mentioned that the very fine crystallite sizes considerably broaden the XRD pattern (Fig. 5) and XRD observations need to be completed with HRTEM observations to conclude on the structural organization evolution in the temperature range 1400–1800 °C under nitrogen. HRTEM are under investigations.

4. Conclusions

In the present study, our main motivation was to investigate the high temperature thermal behavior of BN nanoparticles ($B_{1.0}N_{0.9}$ -NPs) produced by spray-pyrolysis of borazine at 1400 °C. We observed that $B_{1.0}N_{0.9}$ -NPs are relatively stable in air below 850 °C in which only oxidation of the NP surface proceeded. At 850 °C, they started to react most probably due to bulk oxidation.

Under nitrogen, they appeared to be less stable than plate-like BN synthesized from borazine at 1400 °C through conventional pyrolysis. This is mainly due to the spray-pyrolysis (SP) process which is used to produce $B_{1.0}N_{0.9}$ -NPs. They are produced with a low crystallization degree that clearly affects their stability. Using a post-pyrolysis treatment at 1400 °C, $B_{1.0}N_{0.9}$ -NPs remained stable up to 1600 °C similarly to plate-like BN. However, above 1600 °C, a relatively fast weight loss occurred for $B_{1.0}N_{0.9}$ -NPs, whereas plate-like BN remained stable, indicating that their lower size also affects their high temperature thermal behavior.

Acknowledgment

The authors gratefully acknowledge Sylvie Foucaud from SPCTS (Limoges, France) for providing nanoparticles.

References

- Paine RT, Narula CK. Synthetic routes to boron nitride. *Chem Rev* 1990;**90**:73–91.
- Miele P, Bernard S, Cornu D, Toury B. Recent development in polymer-derived ceramic fibers. (PDCFs): preparation, properties, applications—a review. *Soft Mater* 2006;**4**:249–86.
- Iltis A, Maguier C. Eur. Patent 396,448, July 11, 1990.
- Boulanger L, Andriot B, Cauchetier M, Willaime F. Concentric shelled and plate-like graphitic boron nitride nanoparticles produced by CO₂ laser pyrolysis. *Chem Phys Lett* 1995;**234**:227–32.
- Costa J, Sardin G, Campmany J, Bertran E. Preparation of nanoscale amorphous silicon based powder in a square-wave-modulated RF plasma reactor. *Vacuum* 1994;**45**:1115–7.
- Wood GL, Janik JF, Visi MZ, Schubert DM, Paine RT. New borate precursors for boron nitride powder synthesis. *Chem Mater* 2005;**17**:1855–9.
- Tang C, Bando Y, Huang Y, Zhi C, Golberg D. Synthetic routes and formation mechanisms of spherical boron nitride nanoparticles. *Adv Funct Mater* 2008;**18**:3653–61.
- Shi X, Wang S, Yang H, Duan X, Dong X. Fabrication and characterization of hexagonal boron nitride powder by spray drying and calcining–nitriding technology. *J Solid State Chem* 2008;**181**:2274–8.
- Raidongia K, Gomathi A, Rao CNR. Synthesis and characterization of nanoparticles, nanotubes, nanofibers, and graphene-like structures of boron nitride. *Isr J Chem* 2010;**50**:399–404.
- Lian G, Zhang X, Zhu L, Tan M, Cui D, Wang Q. A facile solid state reaction route towards nearly monodisperse hexagonal boron nitride nanoparticles. *J Mater Chem* 2010;**20**:3736–42.
- Salles V, Bernard S, Li J, Brioude A, Chehaidi S, Foucaud S, et al. Design of highly dense boron nitride by the combination of spray-pyrolysis of borazine and additive-free sintering of derived ultrafine powders. *Chem Mater* 2009;**21**:2920–9.
- Zagayansky IL, Samsonov GV. The problem of the oxidizability of boron nitride. *J Appl Chem USSR* 1952;**25**:629–30.
- Coles NG, Glasson DR, Jayaweera SAA. Formation and reactivity of nitrides III. Boron, aluminum, and silicon nitrides. *J Appl Chem* 1969;**19**:178–81.

14. Lyutaya MD, Chernysh IG, Frenkel OA. Chemical properties of nitrides of the a(III)B(V) type. *Sov Powder Metall* 1970;**6**:503–8.
15. Podobeda LT, Tsapuk AK, Buravov AD. Oxidation of boron nitride under nonisothermal conditions. *Sov Powder Metall* 1976;**9**:44–7.
16. Pechentkovskaya LE, Nazarchuk TN. Effect of different crystal structures of boron nitride on its high-temperature stability in oxygen. *Sov Powder Metall* 1981;**7**:83–6.
17. Oda K, Yoshio T. Oxidation kinetics of hexagonal boron nitride powder. *J Mater Sci* 1993;**28**:6562–6.
18. Lavrenko VA, Alexeev AF. High-temperature oxidation of boron nitride. *Ceram Int* 1986;**12**:25–31.
19. Cofer CG, Economy J. Oxidative and hydrolytic stability of boron nitride—a new approach to improving the oxidation resistance of carbonaceous structures. *Carbon* 1995;**33**:389–95.
20. Matsuda T. Stability to moisture for chemically vapour-deposited boron nitride. *J Mater Sci* 1989;**24**:2353–8.
21. Jacobson N, Farmer S, Moore A, Sayir H. High-temperature oxidation of boron nitride: I monolithic boron nitride. *J Am Ceram Soc* 1999;**82**:393–8.
22. Hannache H, Quenisset JM, Naslain R, Heraud L. Composite materials made from a porous 2D-carbon-carbon preform densified with boron nitride by chemical vapour infiltration. *J Mater Sci* 1984;**19**:202–12.
23. Shieh MD, Lee C. A more general structural model which includes the induction time for gas–solid reactions II. The kinetics of alpha-boron nitride oxidation. *Chem Eng Sci* 1993;**48**:1851–7.
24. Gogotsi YG, Lavrenko VA. *Corrosion of High-Performance Ceramics*. Berlin, Heidelberg: Springer-Verlag; 1992.
25. Chase Jr MW, Davies CA, Downey Jr JR, Frurip DJ, MacDonald RA, Syverud AN. In the 3rd edition of the American Chemical Society and American Physical Society, NY, 1986.
26. Yan XB, Gottardo L, Bernard S, Dibandjo P, Brioude A, Moutaabbid H, et al. Preparation of silicoboron carbonitride materials via polymer nanocasting. *Chem Mater* 2008;**20**:6325–34.
27. Li J, Bernard S, Salles V, Gervais C, Miele P. Preparation of polyborazylene-derived bulk boron nitride with tunable properties by warm-pressing and pressureless. *Pyrolysis Chem Mater* 2010;**22**:2010–9.
28. Duperrier S, Gervais C, Bernard S, Cornu D, Babonneau F, Miele P. Controlling the chemistry, morphology and structure of boron nitride-based ceramic fibers through a comprehensive mechanistic study of the reactivity of spinnable polymers with ammonia. *J Mater Chem* 2006;**16**:3126–38.
29. Bernard S, Fiaty K, Miele P, Cornu D, Laurent P. Kinetic modelling of the polymer-derived ceramics (PDCs) route: investigations of the thermal decomposition kinetics of poly[B-(methylamino)borazine] precursors into boron nitride. *J Phys Chem B* 2006;**110**:9048–60.
30. Bechelany M, Brioude A, Stadelmann P, Bernard S, Cornu D, Miele P. Preparation of BN micro/nanotubes with a unique chemical process. *J Phys Chem C* 2008;**112**:18325–30.
31. Toutois P, Miele P, Jacques S, Cornu D, Bernard S. Structural and mechanical behavior of boron nitride fibers derived from poly[(methylamino)borazine] precursors: optimization of the curing and pyrolysis procedures. *J Am Ceram Soc* 2006;**89**:42–9.
32. Janakiraman N, Weinmann M, Schuhmacher JK, Müller K, Bill J, Aldinger F. Thermal stability phase evolution, and crystallization in Si–B–C–N ceramics derived from a polyborosilazane precursor. *J Am Ceram Soc* 2002;**85**:1807–14.